



Multibody Dynamics Analysis of A V-6 Engine

Mushtaq Ahmad Shah¹, Dr. Roopesh Tiwari²

¹Research Scholar, ²Associate Professor,
Mechanical Engineering Department, IET, SAGE University, Indore

ABSTRACT

Automobile is one of the most used transportation media and so engineers are continuously trying to make it more and more efficient. The moving parts of engine create noise/vibration. When the level of noise is more it disturbs the comfort of the rider. As a consequence of increased vibration the parts are acted upon by extra forces causes worn out before time. The primary objective of this work is to analyse the forces on movable parts. To know critical forces that are being acted during the combustion cycle Multibody Dynamics (MBD) is carried out. The analysis will help in modifying the design so that the noise and vibration produced are lower down to a considerable level.

Keyword:Automobile, Engine, Noise, Vibration, MBD

Introduction

Noise and vibration (NV) is one of the critical fields of automobiles that need to be taken care seriously. The major source of NV is engine. When the level of noise is more it disturbs the comfort of the rider and it causes anxiety to the persons using that vehicle. As a consequence of increased vibration the parts get worn out before time. It is very difficult to diagnose NV problems for a vehicle. The major issue is to have same running conditions/environment every time when it is being tested. It is better to simulate the conditions in which the problem actually generated. For this a model is required to confirm the root cause and recognize a solution to the problem. Then the solutions can be applied to the complaint vehicle for verification. So now the result will be depended of correctness of assumptions made during the modeling of each part and assembling too. It will be more significant for assuming/simulating the conditions of impact/ vibration paths.

Literature Review

The branch of engineering that measures and modifies the parameters of noise as well as vibration of an automobile for example bus and car is called as Noise/Vibration/Harshness, in short NVH and N & V. The term harshness is being generally misused. Furuhashi S and Hirukawa K, did an experiment related to generating vibration using a undersized hammer side by side of point T4 with engine off position. The result of experiment shows that piston slap shock in a diesel engine causes considerable noise in its idling condition. Anastasios Zavos, Pantelis G Nikolakopoulos, presented a thorough experimental study of piston assembly friction and noise in a single-cylinder motorbike engine operating at low speeds. The friction of the piston ring pack is evaluated using a foil strain gauge with minimal cylinder modification on the thrust side. Nayak, N., Reddy, P., Aghav, Y., Sohi, N. et al., studied piston slap in single cylinder high-powered engine, which showed large vibrations and noise during the field trials. Fabi, P., Flekiewicz, M., Madej, H., Wojnar, G. et al. (2007), has presented influence of piston skirt clearance on engine noise. LeiLi, Yufan Zheng, MaolinYang et al. (2020), did a survey that briefly reviews feature modeling historical evolution first. Subsequently, various approaches to resolving the interoperability issues during product lifecycle management are reviewed.

Multibody Dynamics

It involves the exploration of the dynamic behaviour of interconnected bodies having vast translational and rotational displacements. MBD is a one of the well recognized simulating tools. It can be used for the simulation of structures and mechanisms which exemplify nonlinearity, large deflections, backlash etc. The tool proposes a number of predefined terms, and linear and non-linear connections etc. When the ICE is up and running because if the mechanical components working to carry on the combustion cycles some forces are generated which in turn effects and N&V levels of the engine. These forces are can also be one of the reasons for failure of the components at some stages. To know some important forces that are being acted during the combustion cycle MBD is carried out. Altair Inspire motion is used to carry out the MBD of ICE.

Preprocessing

To carry out the analysis in inspire motion contacts, connections, couplings, actuators and rigid groups in order to define working of various components more precisely.

• **Input**

To rotate the crank shaft in order to resemble the motion during a combustion cycle motor (Fig 1) is given as an input with a max RPM of 6000. We have considered 6000 as our input value because it's in the mean rpm range so that we can get more accurate results.

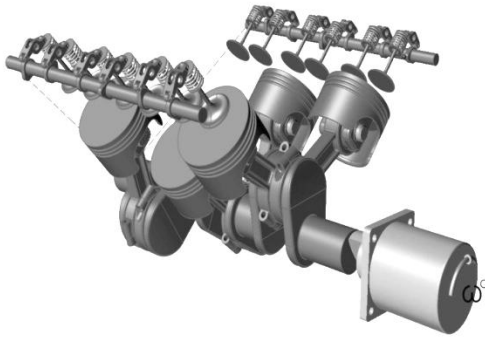


Fig 1: Motor connected to crankshaft

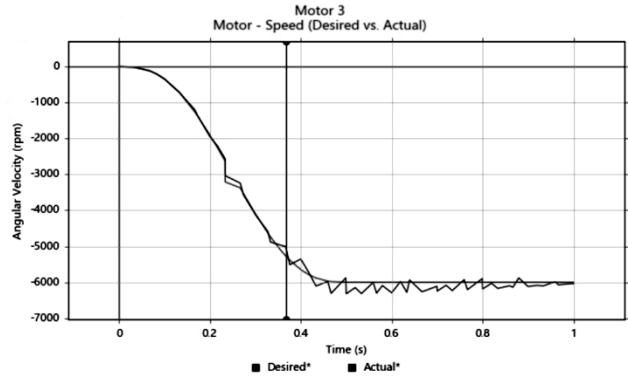


Fig 2: Moto Desired v/s actual rpm

The curve (Fig 2) shows the actual rpm which is reduced compared to desired rpm due to losses In engine.

• **Gravity**

Gravity condition is defined in order to replicate more precise physical model is shown in Figure 3.

• **Actuators**

A mechanical actuator functions to execute movement by converting one kind of motion such as rotary motion into another kind of motion such as translating motion. An example of such actuator is Crankshaft and connecting rod. This is implementing into the analysis to make it more accurate and

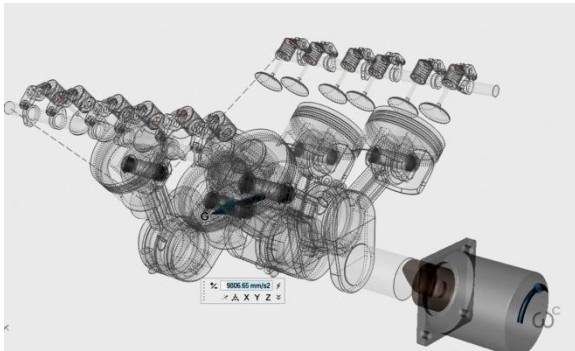
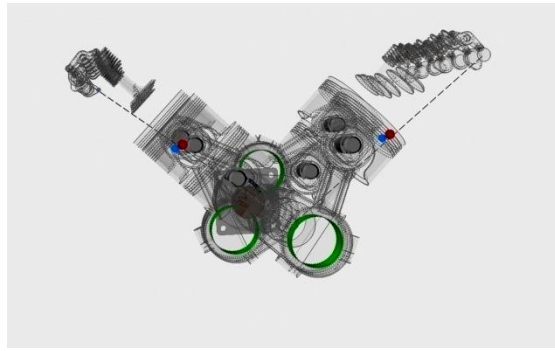


Fig 3: Gravity



get a precise result

Fig 4: coupling

• **Coupling**

A coupling (Fig 4) condition generally couples/links two or more components in order to make then dependent to one another. In this analysis both camshaft and crankshaft are coupled in order to replicate the timing mechanism for proper movement of the components

Table 4.1: Inputs for coupling

Name	Entities	Joint 1 Coupling	Scale 1	Joint 2 Coupling	Scale 2	Reverse Direction
Coupler 3	Joint.264, Joint.265	Rotational	360 deg	Rotational	180 deg	<input type="checkbox"/>
Coupler 4	Joint.264, Joint.262	Rotational	360 deg	Rotational	180 deg	<input type="checkbox"/>

• **Rigid Groups**

Rigid groups resemble the components that are rigid and cannot move. In this analysis rigid groups are provided for two reasons

- To define the components which are actually rigid
- To calculate the forces acting on the components.

The rigid connections are given in order to calculate the forces and various parameters they are related to the valve and springs

• **Contacts**

Contacts resemble the relation between two components which are in a way that they both touch each other. Contacts are giving as an input in this

analysis to resemble more precise physical model.

• **Joints**

Joints are applied in order to define the components such that a more accurate resemblance to physical model is created, refer Table 1. Simulation is carried out for a time period of 2 sec in order to obtain the intended result.

• **Piston**

After the simulation is completed displacement and joint force at piston is noted down. For reference purpose results at 2 pistons out of 6 are considered.

The graph (Fig 5) shows time vs. piston force curve, peak value and low FM= 140000N at 0.53s, FZ=60000N at 0.44s, FY= 60000N at0.82s. The graph (Fig 6) shows time vs. piston force curve, peak value and low FM= 100000N at 0.0.46s, FZ=52000N at 0.42s.

Table: 1 Type of joints

Name	Connection Type	Parts	State	Detected Features	Search Distance	Material	Behavior
Joint 186	Pin	rocker_arm,rocker_arm.	Active	Aligned Holes	0 mm	Steel (AISI 304)	Default
Joint 188	Pin	rocker_arm,rocker_arm.	Active	Aligned Holes	0 mm	Steel (AISI 304)	Default
Joint 190	Pin	rocker_arm,rocker_arm.	Active	Aligned Holes	0 mm	Steel (AISI 304)	Default
Joint 190	Pin	rocker_arm,rocker_arm.	Active	Aligned Holes	0 mm	Steel (AISI 304)	Default
Joint 191	Pin	rocker_arm,rocker_arm.	Active	Aligned Holes	0 mm	Steel (AISI 304)	Default
Joint 192	Pin	rocker_arm,rocker_arm.	Active	Aligned Holes	0 mm	Steel (AISI 304)	Default
Joint 192	Pin	rocker_arm,rocker_arm.	Active	Aligned Holes	0 mm	Steel (AISI 304)	Default
Joint 193	Pin	rocker_arm,rocker_arm.	Active	Aligned Holes	0 mm	Steel (AISI 304)	Default
Joint 194	Pin	rocker_arm,rocker_arm.	Active	Aligned Holes	0 mm	Steel (AISI 304)	Default
Joint 194	Pin	rocker_arm,rocker_arm.	Active	Aligned Holes	0 mm	Steel (AISI 304)	Default
Joint 195	Pin	piston_head,piston_rod.	Active	Aligned Holes	0 mm	Steel (AISI 304)	Default
Joint 195	Pin	rocker_arm,rocker_arm.	Active	Aligned Holes	0 mm	Steel (AISI 304)	Default
Joint 196	Pin	piston_head,piston_rod.	Active	Aligned Holes	0 mm	Steel (AISI 304)	Default
Joint 196	Pin	rocker_arm,rocker_arm.	Active	Aligned Holes	0 mm	Steel (AISI 304)	Default
Joint 196	Pin	rocker_arm,rocker_arm.	Active	Aligned Holes	0 mm	Steel (AISI 304)	Default
Joint 197	Pin	piston_head,piston_rod.	Active	Aligned Holes	0 mm	Steel (AISI 304)	Default
Joint 197	Pin	rocker_arm,rocker_arm.	Active	Aligned Holes	0 mm	Steel (AISI 304)	Default
Joint 198	Pin	piston_head,piston_rod.	Active	Aligned Holes	0 mm	Steel (AISI 304)	Default
Joint 198	Pin	rocker_arm,rocker_arm.	Active	Aligned Holes	0 mm	Steel (AISI 304)	Default
Joint 199	Pin	piston_head,piston_rod.	Active	Aligned Holes	0 mm	Steel (AISI 304)	Default

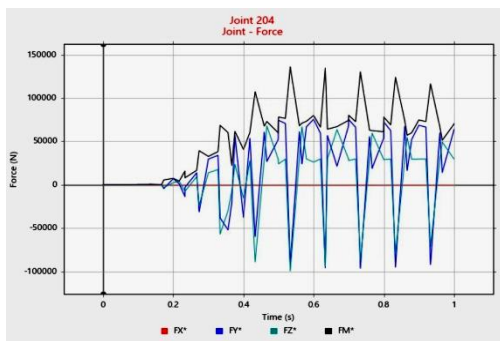


Fig 5: Piston Force-1

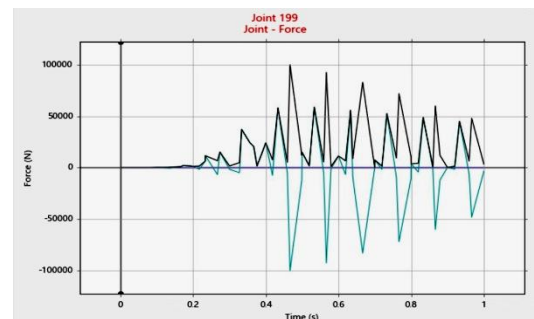


Fig 6 ; Piston Force-2

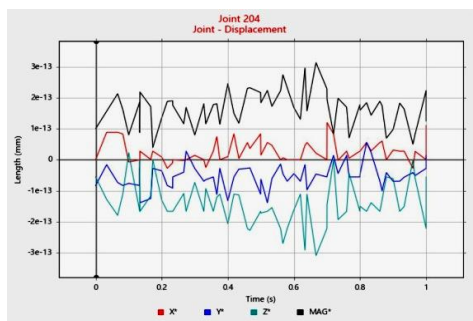


Fig 7: Piston Displacement-1

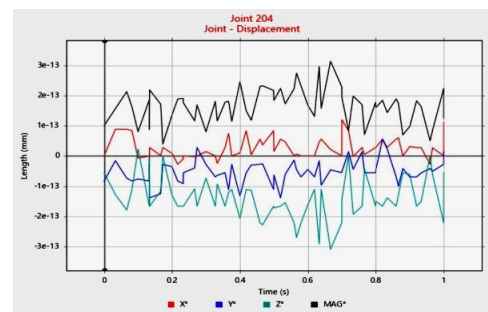


Fig 8: Piston-2 Displacement-2

The graph (Fig 7) shows time vs. displacement curve, peak value X= 1.2e-13mm at 0.72s, Y=0.5e- 13mm at 0.82s, Z= 0.1e-13mm at0.15s. The graph (Fig 8) shows time vs. displacement curve, peak value X= 1.2e-13mm at 0.72s, Y=0.5e- 13mm at 0.82s, Z= 0.1e-13mm at 0.15s.

• **Motor**

As input rpm is given to the crankshaft there is a torque generated at the crankshaft with this we can validate the design of the crankshaft

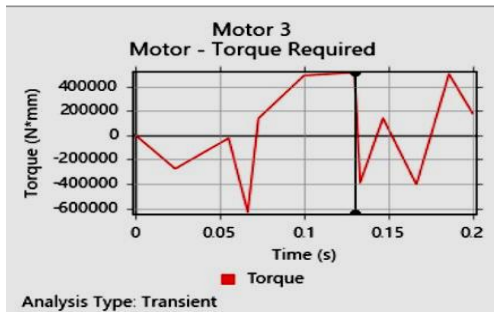


Fig 9: Motor torque

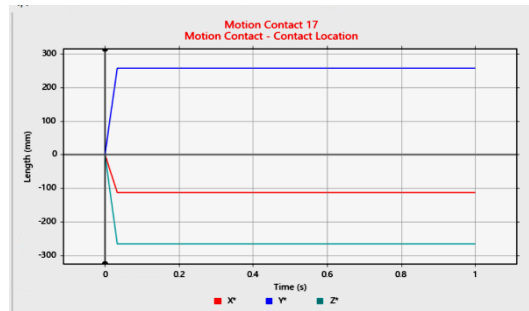


Fig 10: Roller contact location-1

The graph (Fig 9) shows time vs. torque curve, peak value of torque=40*104 mm.

• **Roller**

The forces at roller which is a part of the rocker arm are noted down. This part is taken into consideration because it is continuously in contact with the valve spring on one side and cam on other side and is subjected to loads. After simulation three rollers out of six are taken into consideration in order to represent the more accurate results. From the results it can be said that the roller is subjected to a normal force in the range of 60-100N. The graph (Fig 10) shows length time vs. (displacement) time of roller at input loads, X =110 mm, Y = 260 mm and Z = 270 mm

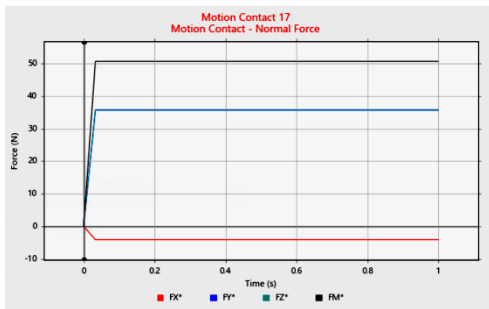


Fig 11: Roller normal force-1

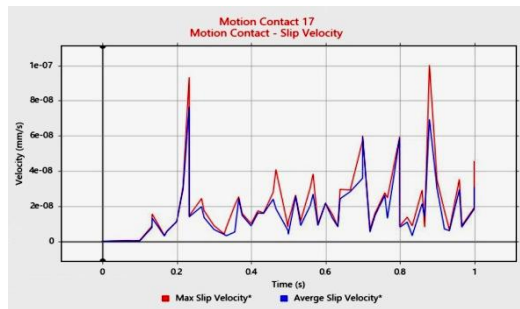


Fig 12: Roller Slip velocity -1

The graph (Fig 11) shows time vs. length (displacement) of roller at input loads, FX = 4mm, FY = 36 mm and FZ = 51 mm. The graph (Fig 12) shows time vs. roller slip velocity (mm/s) of roller at input loads, Mass slip velocity = 1e-07 mm/s at 0.84s, Average Slip Velocity = 7.8e-08 mm/s.

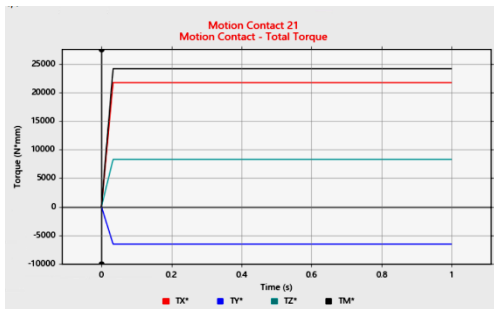


Fig 13: Roller Total torque-1

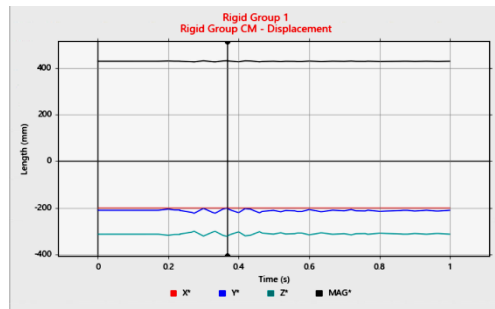


Fig 14: Roller Displacement-1

This graph (Fig 13) shows time vs. Roller torque (N/mm) of roller at input loads ,TX=24000 N/mm, TY=6000N/mm and TZ=8000N/mm , TM=24900N/mm.

• **Valves**

With rigid connection given the forces and other parameters at the valves of the engine are noted. For accurate representation of the results 3 valves out of 12 are taken into consideration. With simulation being completed the results are noted and it can be observed that the displacement is in the range of 0-400mm. This graph (Fig 14) shows time vs. length (displacement) of roller at input loads, X=200mm, Y=200mm, Z=300mm and MAG =410mm.

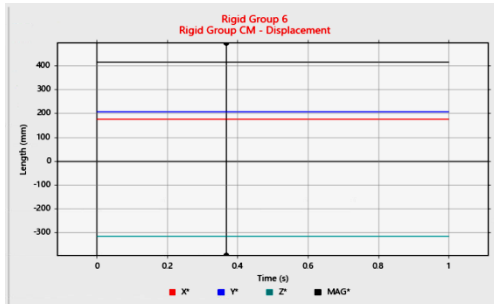


Fig 15: Roller Displacement-2

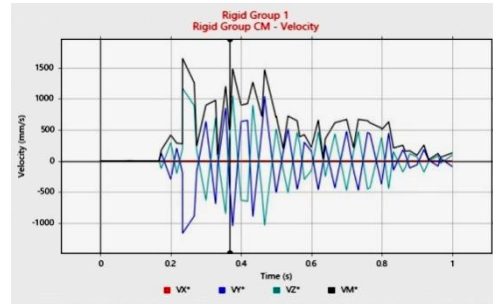


Fig 16: Roller velocity-1

This graph (Fig 15) shows time vs. length (displacement) of roller at input loads, X=180mm, Y=200mm, Z=310mm and MAG =410mm. This graph (Fig 16) shows time vs. velocity (mm/s) of roller at input loads, VX=0mm/s, VY=950mm/s, VZ=1200mm/s and VM =1700mm/s.

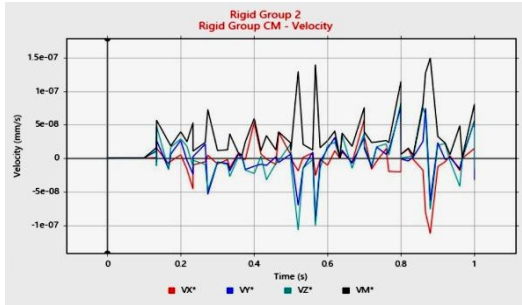


Fig 17: Roller velocity-2

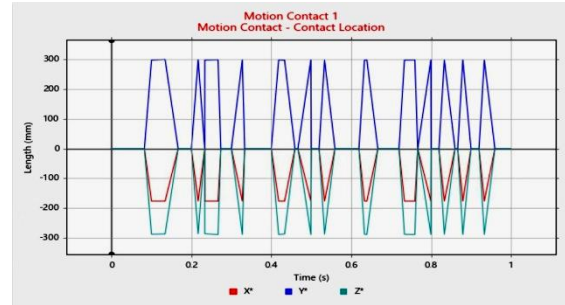


Fig 18: Cam contact location-1

This graph (Fig 17) shows time vs. velocity (mm/s) of roller at input loads, VX=5.1e-08mm/s, VY=7.5e-08mm/s, VZ=4.8e-08mm/s and VM =1.5e-07mm/s

• **Cam**

The cam is one of the major components that is subjected to high deformation as it rotates in higher speeds. 3 cams are chosen out of the 12 in order to represent the solution more accurately. With simulation being completed the results are taken and it can be observed that the max normal force that is exerted on the cam is most likely to be in the range of 8e+4 to 10e+4. This graph (Fig 18) shows time vs. length (displacement) of cam at input loads, X=184mm, Y=300mm, Z=290mm

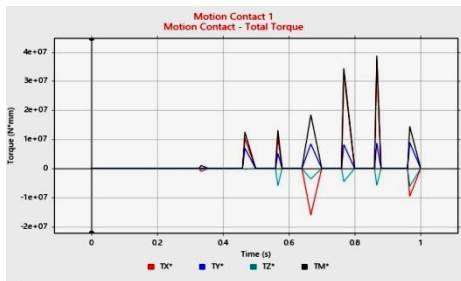


Fig 19: Cam torque-1

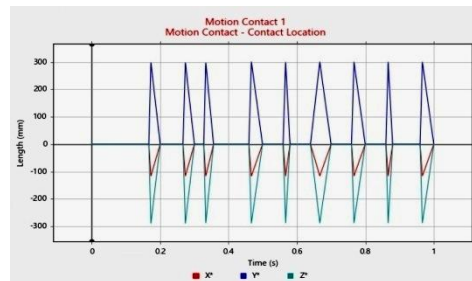


Fig 20: Cam contact location-2

This graph (Fig 19) shows time vs. torque of roller at input loads, TX = 1.6e + 07N/mm, TY = 0.8e+07N/mm, TZ = 0.5e+07N/mm and TM =3.9N/mm. This graph (Fig 20) shows time vs. length (displacement) at cam contact at input loads, X=120mm, Y=300mm, Z=296mm.

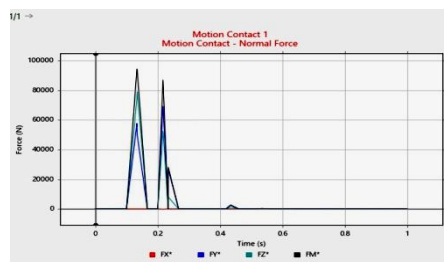


Fig 21: Cam normal force-1

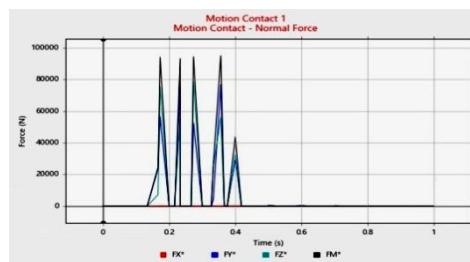


Fig 22: Cam normal force-2

This graph (Fig 21) shows time vs. Normal force of cam at input loads, FX=0mm, FY=57000N, FZ=80000N and FM=86000N. This graph (Fig 22)

shows time vs. Normal force of cam at input loads, FX=0mm, FY=78000N, FZ=76000N and FM=86000N

Coil spring

When the engine in up and running the coil springs which are placed in between roller of rocker arm and valve are subjected to compressions and it is important. This result can help is validating the design of the spring and examine the forces and other parameters related to the spring

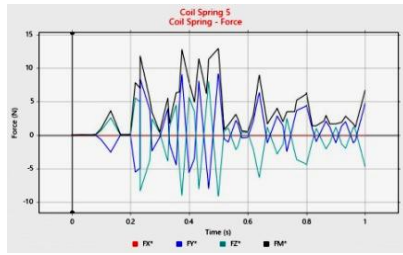


Fig 23: Coil spring Force-1

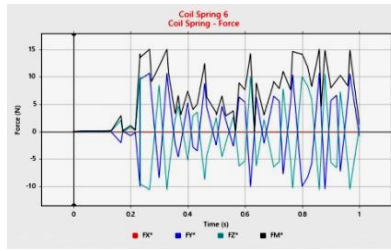


Fig 24: Coil spring Force-2

This graph (Fig 23) shows time vs. Normal force of coil spring at input loads, FX=0mm, FY=9N, FZ=7N and FM=13.7N. This graph (Fig 24) shows time vs. Normal force of coil spring at input loads, FX=0mm, FY=10N, FZ=10N and FM=15N.

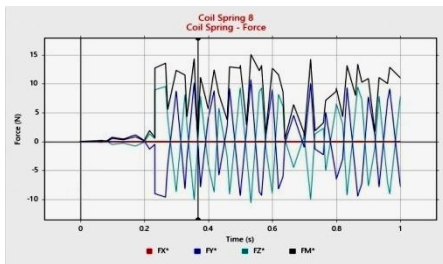


Fig 25: Coil spring Force-3



Fig 26: Coil spring free length vs length-1

The graph (Fig 25) shows time vs. Normal force of coil spring at input loads, FX=0mm, FY=10N, FZ=9N and FM=15N. This graph (Fig 26) shows coil spring free length vs. time of coil spring at input loads, and Free length = 44mm at 0.45s, length=28mm constant. The graph (Fig 27) shows time vs. displacement of coil spring at input loads, peak value =13mm at 0.27s and Min. value=-2mm at 0.69s. This graph (Fig 28) shows coil spring free length vs. time of coil spring at input loads, and Free length=44mm at 0.45s, length=28mm constant.

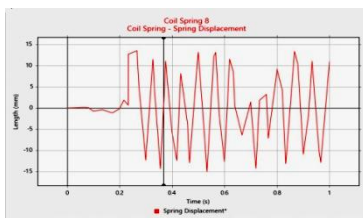


Fig 27: Coil spring displacement-1

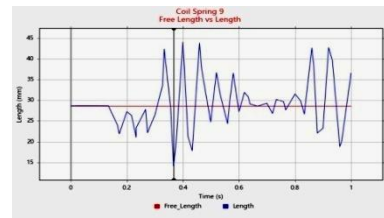


Fig 28: Coil spring free length vs length-2

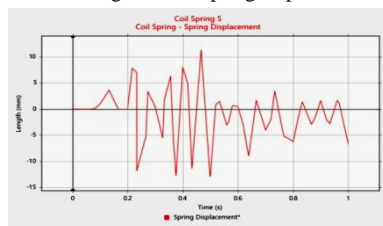


Fig 29: Coil spring displacement -2

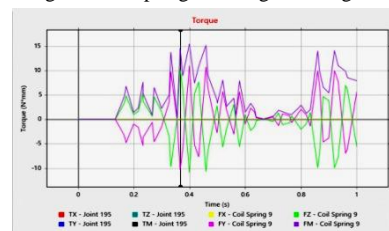


Fig 30: Joints type

This graph (Fig 29) shows time vs. displacement of coil spring at input loads, peak value =13mm at 0.47s and Min. value=-2mm at 0.58s.

1. Theoretical Calculations

Piston slaps force: The equation for piston slap force is as follows:

$$A = \frac{m_p(-r\theta^2 \sin \beta - \phi \ddot{L})}{\cos \phi} + \frac{m_r b(-r\theta^2 \sin \beta - \phi b) \ddot{L}_o \ddot{\phi}}{L \cos \phi}$$

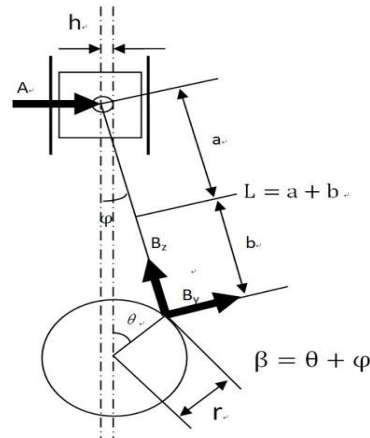


Fig 31: Dimensional notations of piston

Most of the variables used are as defined in figure 1. The other variables used are as follows:

m_p = mass of the piston assembly, including the wristpin if it is a pressed pin

m_r = mass of the connecting rod assembly, including the wristpin if it is a floating pin

b = distance from the connecting rod centre of gravity to the crankpin centreline

I_o = mass moment of inertia of the connecting rod assembly about the centre of gravity M_{in}

$$B_y = \left[\frac{m_r a}{L(-r\ddot{\theta}^2 \sin \beta - \dot{\varphi} \ddot{b})} + \frac{I_o \ddot{\varphi}}{L} \cos \varphi - [m_p(-r\ddot{\theta}^2 \sin \beta \tan \varphi - r\ddot{\theta}^2 \cos \beta - \dot{\varphi} L \tan \varphi - \varphi^2 L) + m_r \left(-\frac{rb}{L\ddot{\theta}^2 \sin \beta \tan \varphi} - r\ddot{\theta}^2 \cos \beta - \frac{\dot{\varphi} b^2}{L \tan \varphi} - \varphi^2 b \right) - I_o \ddot{\varphi} \sin \varphi / L \cos \varphi] \cos \varphi + m_r b r \ddot{\theta}^2 / L \right]$$

$$B_z = \left[\frac{m_r a}{L(-r\ddot{\theta}^2 \sin \beta - \dot{\varphi} \ddot{b})} + \frac{I_o \ddot{\varphi}}{L} \sin \varphi - [m_p(-r\ddot{\theta}^2 \sin \beta \tan \varphi - r\ddot{\theta}^2 \cos \beta - \dot{\varphi} L \tan \varphi - \varphi^2 L) + m_r \left(-\frac{rb}{L\ddot{\theta}^2 \sin \beta \tan \varphi} - r\ddot{\theta}^2 \cos \beta - \frac{\dot{\varphi} b^2}{L \tan \varphi} - \varphi^2 b \right) - I_o \ddot{\varphi} \sin \varphi / L \cos \varphi] \cos \varphi + m_r b r \ddot{\theta}^2 \cos \theta / L \right]$$

Conclusion

IC engines are one of the critical parts that create a large amount of noise and vibration in an automobile. These forces are generated due to the combustion cycle. As a consequential effect, these forces cause failure of the components. In this paper, an effort is made to carry out MBD to know some important forces that are being acted during the combustion cycle.

References

1. Anastasios Zavos, Pantelis G Nikolakopoulos, (2017) Measurement of friction and noise from piston assembly of a single-cylinder motorbike engine at realistic speeds, Proceedings of the Institution of Mechanical Engineers, Part D: Journal of Automobile Engineering ISSN: 0954-4070.
2. Nayak, N., Reddy, P., Aghav, Y., Sohi, N. et al., "Study of Engine Vibration Due to Piston Slap on Single Cylinder High Powered Engine," SAE Technical Paper 2005-26-046, 2005, <https://doi.org/10.4271/2005-26-046>.
3. Fabi, P., Flekiewicz, M., Madej, H., Wojnar, G. et al., "Influence of Piston Slap on Engine Block Vibration," SAE Technical Paper 2007-01-2163, 2007, <https://doi.org/10.4271/2007-01-2163>.
4. LeiLi, Yufan Zheng, MaolinYang, JiewuLeng, Zhengrong Cheng, Yanan Xie, Pingyu Jiang, Yongsheng Ma, A survey of feature modeling methods: Historical evolution and new development Robotics and Computer-Integrated Manufacturing, Volume 61, February 2020, 101851
5. Kelly P, Biermann J W, Using Taguchi methods to aid understanding of a multi-body clutch pedal noise and vibration phenomenon, Multi-Body Dynamics: Monitoring and Simulation Techniques, Mechanical Engineering Publications Ltd, 2004
6. Gerges S N Y, De Luca J C and Lalor N (2005), 'Effect of cylinder lubrication on piston slap', SAE paper 2005-01-2165.
7. Haddad S D (1995), 'Theoretical treatment of piston motion in IC piston engine for the prediction of piston slap excitation', Mechanism and

Machine Theory, 30(2), 253–269.

7. Doğan, S. N.; Ryborz, J.; Bertsche, B.: Rattling and Clattering Noise in Automotive Transmissions – Simulation of Drag Torque and Noise, Symposium – Transient Processes in Tribology, Leeds–Lyon Symposium, Lyon, September 2003.
8. Cheng Z, Analysis of Automobile Crash Response Using Wavelets, SAE Paper 2002-01 0183, 2002.